Advances Toward Ge/SiGe Quantum-Well Waveguide Modulators at 1.3μm

Mohamed-Saïd Rouifed, Delphine Marris-Morini, Papichaya Chaisakul, Jacopo Frigerio, Giovanni Isella, Daniel Chrastina, Samson Edmond, Xavier Le Roux, Jean-René Coudevylle, David Bouville, and Laurent Vivien

I. Introduction

SILICON photonics has generated an increasing interest in recent years. Both microelectronics and telecommunications could benefit from the development of low cost and high performance solutions for high-speed integrated optical links [1], [2]. Optoelectronic devices for integrated transceivers including sources, modulators and detectors are the subjects of intense research. Silicon modulators based on carrier depletion have recently achieved high performances such as 40 Gb/s operation with high extinction ratio (ER) and low loss [3]. Silicon Mach Zehnder modulators are interesting for telecommunication applications but their energy consumption of a few pJ/bit is prohibitive for inter- and intra-chip optical communications. For such short optical link applications, energy consumption of the optical modulators is a major concern [4]. In this context Ge-rich Ge/SiGe quantum wells (QWs) are promising for compact and low power consumption electro-absorption modulators [5]. Using a 3-μm-wide and 90-μm-long Ge/$Si_{0.15}Ge_{0.85}$ QWs waveguide, a 23 GHz electroabsorption modulator has been experimentally demonstrated, exhibiting an ER higher than 10 dB over a wide spectral range around 1.45 μm [6]. Different methods have been proposed to tune the operating wavelength of QCSE in Ge/SiGe QWs to 1.3 or 1.55 μm, such as strain-engineering [7], [8], and have been experimentally verified [9]–[12]. In surface illuminated devices the quantum-confined Stark effect (QCSE) has been already demonstrated at the wavelength of 1.3 μm. Such operating wavelength, which is shorter than the 1.4 μm absorption edge of Ge QWs grown on $Si_{0.1}Ge_{0.9}$ buffers, is achieved thanks to the higher compressive strain imparted to the Ge well by the use of $Si_{0.21}Ge_{0.79}$ virtual substrate (VS) [9], [10]. However, performance of a waveguide modulator at 1.3 μm has not been evaluated so far. Indeed the increased contribution from indirect band-gap absorption at this wavelength could spoil the performances of a waveguide modulator in terms of ER and insertion loss (IL) [13]. This paper reports on the latest advances towards the realization of a Ge/SiGe QW waveguide modulator working at 1.3 μm. Two kinds of waveguide modulators were considered. First, a stand-alone modulator using Ge/$Si_{0.35}Ge_{0.65}$ QWs on top of a 13-μm $Si_{0.21}Ge_{0.79}$ buffer on silicon was fabricated and characterized. Subsequently, aiming at the integration of a Ge/SiGe QW modulator on a silicon-on-insulator (SOI) waveguide, we developed a relaxed buffer with 360 nm thickness that would practically allow the optical coupling between a SOI waveguide and the Ge/SiGe QW active region. Here we present photocurrent measurements from a surface illuminated Ge/$Si_{0.15}Ge_{0.85}$ QW structure grown on top of a 360-nm-thick $Si_{0.08}Ge_{0.92}$ buffer deposited on a silicon wafer and operating at a wavelength around 1.4 μm. This step helped evaluate the effectiveness of such thin buffer for QCSE structure integration on silicon. The promising experimental results led us to model the performances (optical loss, ER and energy per bit) of a QCSE modulator integrated on a SOI waveguide by means of such a thin SiGe buffer and operating at 1.3 μm.

Manuscript received September 9, 2013; revised December 3, 2013; accepted December 3, 2013. This work was supported in part by the French ANR under project GOSPEL (Direct Gap Related Optical Properties of Ge/SiGe Multiple Quantum Wells), in part by the "Institut Universitaire de France," and in part by the European Commission through project Green Silicon. The fabrication of the devices was performed at the nano-center CTU-IEF Minerve, which is partially funded by the "Conseil Général de l'Essonne."

M.-S. Rouifed, D. Marris-Morini, P. Chaisakul, S. Edmond, X. Le Roux, J.-R. Coudevylle, D. Bouville, and L. Vivien are with the Institut d'Electronique Fondamentale, University Paris-Sud, CNRS, 91405 Orsay Cedex, France (e-mail: Mohamed-Said.Rouifed@u-psud.fr; delphine.morini@u-psud.fr; papichaya.chaisakul@u-psud.fr; Samson.edmond@u-psud.fr; Xavier.Leroux@u-psud.fr; jean-rene.coudevylle@u-psud.fr; david.bouville@u-psud.fr; laurent.vivien@u-psud.fr).

J. Frigerio, G. Isella, and D. Chrastina are with the L-NESS, Dipartimento di Fisica del Politecnico di Milano, Polo di Como, I 22100 Como, Italy (e-mail: jacopo.frigerio84@gmail.com; giovanni.isella@polimi.it; danny@chrastina.net).

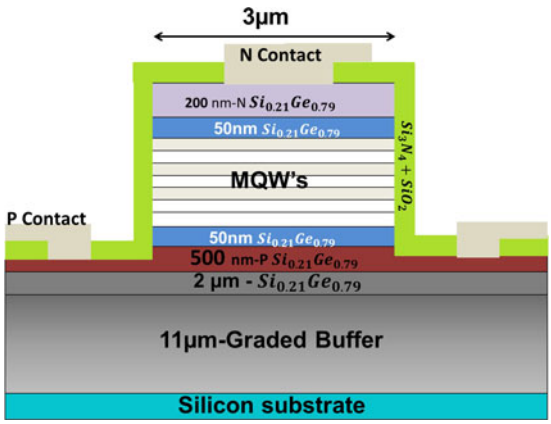

Fig. 1. Cross section of the stand-alone modulator working at 1.3 μm: 20 periods of Ge/$Si_{0.35}Ge_{0.65}$ QWs/barriers embedded in a PIN diode are grown on top of a 11-μm-thick graded buffer followed by a 2-μm-thick constant composition layer.

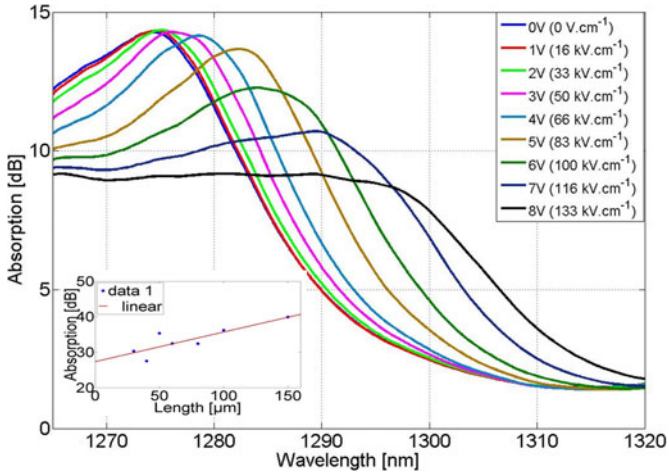

Fig. 2. Experimental absorption spectra of the stand-alone modulator for different applied reverse bias voltages (FP fringes coming from waveguide facets have been filtered out). Inset: absorption as a function of the length of the modulator (cut-back technique) used to remove loss coming from the coupling of light into and out of the tested device.

II. Stand-Alone Modulator at 1.3 μm

A. Design and Fabrication

Ge/SiGe QWs were grown by low-energy plasma-enhanced chemical vapor deposition (LEPECVD) [14]. For the fabrication of the stand-alone modulator, an 11 μm thick $Si_{1-y}Ge_y$ graded buffer was deposited with linearly increasing Ge content from Si to $Si_{0.21}Ge_{0.79}$, capped with a 2-μm-thick $Si_{0.21}Ge_{0.79}$ layer forming a relaxed VS. A 500-nm-thick boron-doped ($\sim 1\times10^{18}$ cm^{-3}) $Si_{0.21}Ge_{0.79}$ layer was grown to serve as a p-type contact, followed by a 50-nm-thick $Si_{0.21}Ge_{0.79}$ spacer. The QW region consists of twenty periods of 8-nm-thick Ge QWs and 12-nm-thick $Si_{0.35}Ge_{0.65}$ barriers, similar to the design used in [9]. The Ge content of the barriers and the VS has been chosen to obtain a strain-balanced design, in which Ge QWs ($Si_{0.35}Ge_{0.65}$ barriers) are compressively (tensile) strained due to the lattice mismatch with the $Si_{0.21}Ge_{0.79}$ VS. Finally, a 50-nm-thick $Si_{0.21}Ge_{0.79}$ cap layer and a 200-nm-thick phosphorus-doped ($\sim 1\times10^{18}$ cm^{-3}) $Si_{0.21}Ge_{0.79}$ layer were added to form the n-contact. The cross section of the fabricated device is shown in Fig. 1.

A 3-μm-wide and 50-μm-long modulator was fabricated in order to investigate the modulation performance of the Ge/$Si_{0.35}Ge_{0.65}$ QWs in a waveguide configuration. The mesa was patterned by ultraviolet (UV) lithography and dry etching. A passivation stack of SiO_2/Si_3N_4 was deposited by plasma enhanced chemical vapor deposition (PECVD). The bottom and top contacts were defined by UV lithography, reactive ion etching, and wet etching of the passivation layer. An Al layer was evaporated and lifted-off for both top and bottom contacts.

B. Characterization

Modulator transmission spectra were measured at room temperature from 1260 to 1320 nm with a wavelength resolution of 0.5 nm. Light from a tunable laser was polarized and butt-coupled into the Ge/SiGe QW modulator using a polarization-maintaining lensed-fiber. TE polarization was chosen according to the polarization dependence of the QCSE in Ge/SiGe structures as investigated in [15]. Light at the output of the modulator was collected by an objective and coupled to an infrared photodetector. Electrical probes were used to apply the bias voltage. Absorption spectra as a function of the wavelength were deduced from the measurements for reverse bias voltages from 0 to 8 V. Fabry-Perot oscillations with a 4 nm free-spectral range were observed and attributed to the cavity formed between the facets of the 50-μm-long waveguide. A low-pass filter was used to remove these oscillations from the recorded experimental measurements. A cut-back technique was used to remove loss coming from the coupling of light into and out of the tested device (inset of Fig. 2). Finally the resulting absorption spectra of the Ge/SiGe QW modulator are reported in Fig. 2.

At 0 V, an absorption peak was found at 1.274 μm (0.972eV), which can be attributed to the excitonic transition between the first valence band heavy hole level (HH1) and the first conduction band state at Γ (cΓ1). By using the Lorentzian function to fit the spectra, the half width at half maximum of the excitonic peak can be estimated to be 8.5 meV. This value is very competitive with previously reported values on similar structures [9], [10] illustrating the good quality of the grown structures. With increasing reverse bias voltages, the two main characteristics of the QCSE were observed around 1.3 μm: the Stark (red) shift of the absorption spectra and the reduction of the exciton peak due to the reduction of the overlap between the electron and hole wavefunctions. Mode calculations were performed using a film mode matching complex solver assuming a linear variation of the refractive index in the graded buffer. The contributions to the optical loss of both the graded buffer and the metal in the absorption spectra reported in Fig. 2 were evaluated to be as low as 0.5 dB.

ERs deduced from the absorption spectra are reported in Fig. 3. From 0 to 7 V, the ER reaches 6 dB at 1.293 μm while an ER larger than 4 dB is obtained for a 15 nm spectral range (see Fig. 3(a)). In Fig. 3(b), the ER is reported as a function of wavelength for swing voltages of 2, 3, and 4 V between 4 and 6 V,

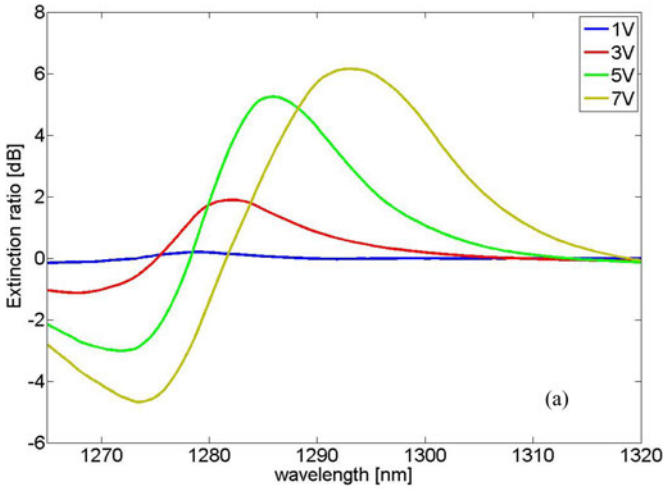

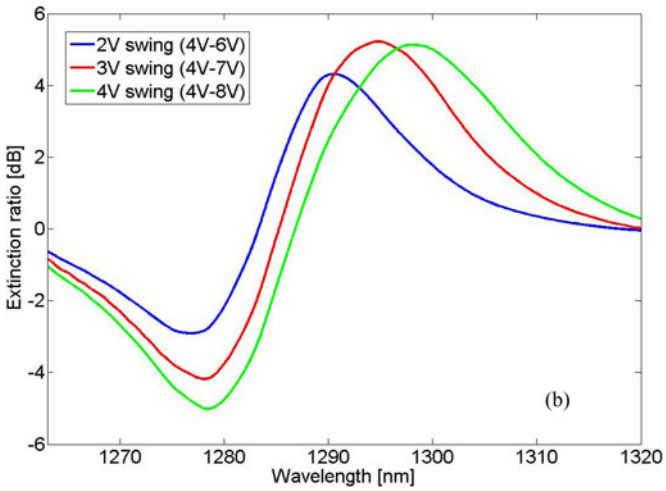

Fig. 3. Extinction ratio of the stand-alone modulator (a) for bias voltages from 0 to 1, 3, 5, and 7 V (b) for 2, 3, and 4 V swing voltages between 4 and 6, 4 and 7, and 4 and 8 V, respectively.

4 and 7 V, and 4 and 8 V, respectively. An ER larger than 4 dB was obtained for 4, 10, and 11 nm spectral ranges for 2, 3, and 4 V swing, respectively. In these spectral ranges, optical loss varies from 6 to 3 dB. Such a Ge/SiGe QW waveguide modulator configuration therefore demonstrates promising performances at wavelengths around 1.3 μm.

III. Toward a Ge QW Modulator Integrated on SOI Waveguide

Silicon photonics is largely based on the use of SOI waveguides, on which active materials such as III–V semiconductors have already been successfully integrated [16].

The first Ge/SiGe QW waveguide modulator monolithically integrated with SOI waveguides through direct-butt coupling and selective epitaxial growth provided 3.2 dB ER optical modulation with a 1 V swing [17]. As a second option, evanescent vertical coupling has been proposed as an efficient way to couple light from the SOI waveguides to the Ge/SiGe QW active regions [18], [19]. Such a coupling approach requires dramatic reduction of the buffer thickness from 13 μm down

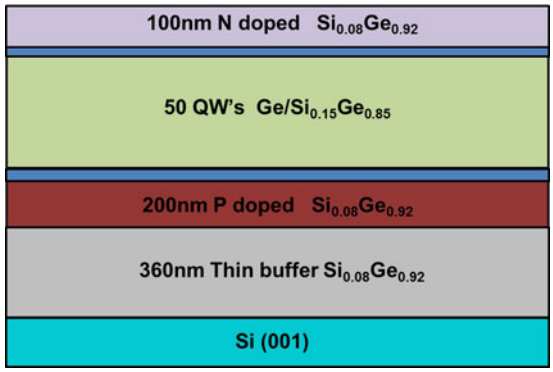

Fig. 4. Cross section of the Ge/SiGe QW structure used to demonstrate QCSE using a thin SiGe buffer on silicon: 50 periods of 10 nm Ge QWs and 14 nm $Si_{0.15}Ge_{0.85}$ barriers were grown on a 360 nm thick $Si_{0.08}Ge_{0.92}$ buffer layer.

to few hundred nanometers. As the buffer thickness reduction and the modification of Ge QWs to operate at 1.3 μm are both very challenging as regards the epitaxial growth, we decided to firstly experimentally evaluate the usability of a 360-nm-thick homogeneous $Si_{0.08}Ge_{0.92}$ buffer on silicon to demonstrate QCSE from 50 Ge/$Si_{0.15}Ge_{0.85}$ QWs. Such a Ge stack is known to exhibit good QCSE behavior [5]. The performances of a Ge/$Si_{0.65}Ge_{0.35}$ QW modulator integrated with a SOI waveguide using a 360-nm-thick buffer and operating at 1.3 μm have then been evaluated theoretically.

A. Ge/SiGe QWs on Thin Homogeneous Buffer on Silicon Substrate

Due to the difference in lattice constants and thermal expansion coefficients between Si and Ge, the epitaxial growth of Ge/SiGe structures on silicon requires the use of a buffer layer (virtual substrate) to trap misfit dislocations and to reduce the threading dislocation density at the growth surface of the quantum well (QW) layers [19]. A 13-μm-thick buffer (see Section II) leads to a fully relaxed VS with a low threading dislocation density without additional annealing. For Ge QW integration on SOI waveguides, such an approach is not possible. We therefore studied the QCSE in a 50 periods Ge/$Si_{0.15}Ge_{0.85}$ QW structure grown on a 360-nm-thick homogeneous $Si_{0.08}Ge_{0.92}$ buffer as shown in Fig. 4. This study was carried out on standard bulk silicon substrates. However no substantial difference is expected for what concerns the epitaxial growth as compared to the deposition on SOI substrate. The 360-nm-thick $Si_{0.08}Ge_{0.92}$ buffer layer was obtained by sequentially growing four 90-nm-thick $Si_{0.08}Ge_{0.92}$ films. Each growth was performed at 400 °C, at a rate of 0.1 nm/s followed by 40 minutes of thermal annealing between 600 and 800 C in order to reduce the dislocation density and to form a relaxed buffer layer. The strain-compensated active region was then grown, beginning with a 200-nm-thick $Si_{0.08}Ge_{0.92}$ boron-doped layer, followed by 50 periods of 10-nm-thick Ge QWs and 14-nm-thick $Si_{0.15}Ge_{0.85}$ barriers. Finally, a 100 nm phosphorus-doped ($\sim 1\times10^{18}$ cm^{-3}) $Si_{0.08}Ge_{0.92}$ layer was added to form an n-type contact. The tested device was a surface illuminated diode patterned by UV lithography and dry etching. Metal contacts were formed by

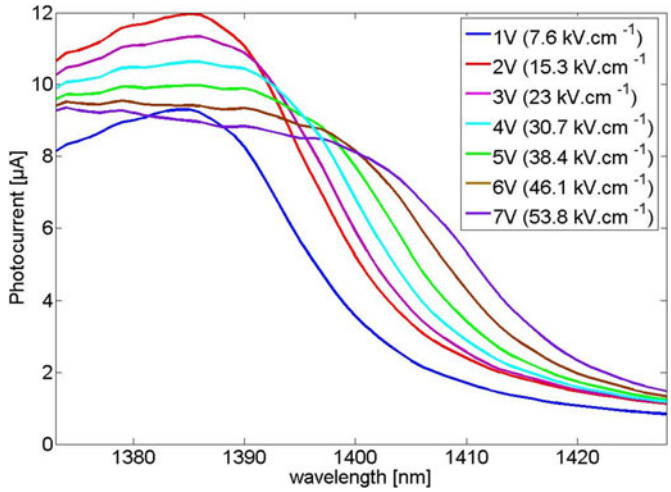

Fig. 5. Photocurrent spectra of the surface illuminated diode made of 50 periods of 10 nm Ge QWs and 14 nm $Si_{0.15}Ge_{0.85}$ barriers grown on a 360 nm thick $Si_{0.08}Ge_{0.92}$ buffer layer.

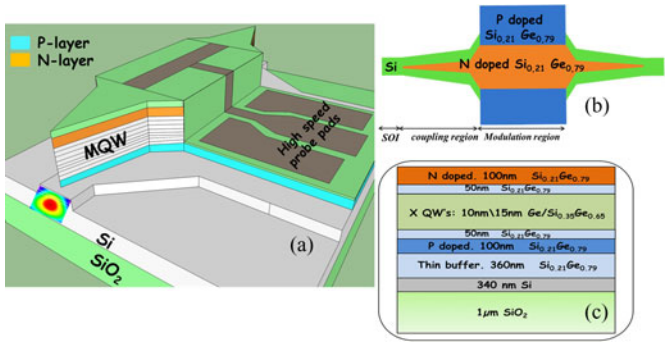

Fig. 6. (a) 3-D view of the simulated device (b) top view and (c) cross view of the QW modulator integrated on SOI.

TABLE I
REFRACTIVE INDEX AND ABSORPTION COEFFICIENT OF THE DIFFERENT LAYERS IN THE SIMULATION

region	n	α
Si	3.5	0
p-doped-$Si_{0.21}Ge_{0.79}$	4.1340	4 cm^{-1}
n-doped-$Si_{0.21}Ge_{0.79}$	4.1340	60 cm^{-1}
$Ge/Si_{0.35}Ge_{0.65}$ QW	4.1346	350 cm^{-1} @ 0V
region		1174 cm^{-1}@ E=83 kV/cm

evaporating 10 nm of Ti followed by 100 nm of Au. Photocurrent measurements were performed at room temperature. Light from a tunable laser was vertically coupled to the device. A chopper and a lock-in amplifier were used to modulate the light intensity and to measure the photocurrent. Quantum confinement at the direct gap of this structure was demonstrated in this device, by the observation of a clear exciton peak attributed to HH1-cΓ1 transition (Fig. 5). From photocurrent measurements it can be noticed that photo-generated carriers cannot be fully collected at bias voltages lower than 2 V. Indeed, the intrinsic region was not fully depleted at low reverse bias voltages, as previously observed when a structure with a large number of QWs (and therefore a thick intrinsic region) has been used [20].

The main characteristics of the QCSE were observed: red shift of the band-edge and decrease in the absorption at the excitonic peak. According to this result, a thin VS with only 360 nm thickness has been successfully developed and high quality Ge/SiGe QWs were grown on it.

B. Simulation of the Performances of Ge QW Modulator Integrated on a SOI Waveguide

The evaluation of the modulator performance requires the design of an efficient optical taper to couple light from the Si waveguide to the Ge/SiGe QWs. Evanescent vertical couplers according to [18], [19] were considered. Simulations were performed using the eigenmode expansion method [21]. Fig. 6 reports (a) 3-D view, (b) top view, and (c) cross section of the active region. The active region was chosen to obtain modulation at 1.3 μm. It was based on 10-nm-thick Ge QWs and 15-nm-thick $Si_{0.35}Ge_{0.65}$ barriers embedded between $Si_{0.21}Ge_{0.79}$ p- and n-doped regions on a $Si_{0.21}Ge_{0.79}$ VS (same QW stack used for the stand-alone modulator in Section II). From the result reported above in Section III-A, a 360-nm-thick homogeneous $Si_{0.21}Ge_{0.79}$ buffer was considered between the SOI waveguide and the $Ge/Si_{0.35}Ge_{0.65}$ active region. Table I reports on the absorption values taken into account in the simulation. The absorption coefficient in the QW region at the wavelength of 1310 nm was extracted from [9] and free carrier absorption in the *p*- and *n*-layers were calculated using the Drude model. As for the SOI dimensions, a 340-nm-thick silicon layer was considered on top of 1 μm SiO_2. The width of the Si waveguide was 700 nm and the etching depth was 100 nm to ensure a single mode condition. Light coupling to the Ge/SiGe QW stack was performed by laterally tapering the Ge/SiGe QW region to adiabatically transfer the optical mode from the silicon waveguide to the active region. A two taper section was used (see Fig. 6). The first section allowed light to be coupled from the silicon waveguide to the QW region. As shown in [18], a smooth taper slope is required to ensure adiabatic coupling. The second section was used to adapt the width of the Ge/SiGe waveguide to the 1 μm-wide active region waveguide. This active region width was chosen to be compatible with the fabrication process. The taper tip has to be as narrow as possible to avoid disruption of the Si waveguide mode. A 120-nm-wide tip was then chosen to be compatible with fabrication tolerances. The output width of the first section of the taper was chosen equal to 260 nm; for this value, the optical mode was then confined in the Ge/SiGe QW region as illustrated in Fig. 7. A critical width of around 230 nm corresponding to the phase matching condition was deduced from the simulations. Simulations have been performed to evaluate the loss of both sections of the taper as a function of the number of Ge/SiGe QWs. The contributions from the first section as a function of its length and for different number of QWs (10, 15, and 20) are reported in Fig. 8. The lowest optical loss was obtained for the thinnest stack (10 QWs), for which shorter taper length can be considered. However it has to be noted that this configuration also corresponds to the smallest

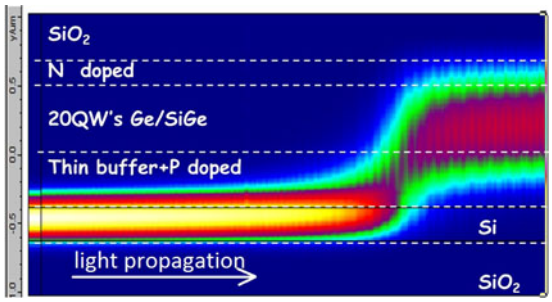

Fig. 7. Electric field intensity profile through a vertical cross section of the first taper, showing the coupling of light from the SOI waveguide to the Ge/SiGe QW region.

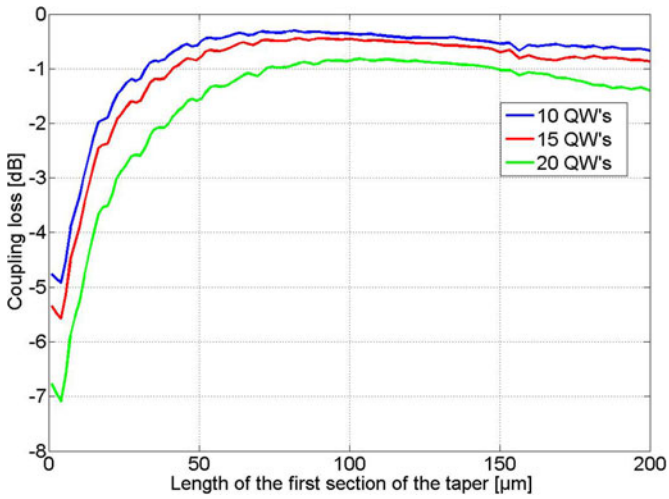

Fig. 8. Coupling loss of the first section of the taper, as a function of its length for different numbers of QWs.

optical mode overlap factor with the QW region. For 10 and 20 QWs structures, an 80-μm-long taper with 0.23 dB loss and 100-μm-long taper with 0.77 dB loss can be used, respectively. As the optical mode confined in Ge/SiGe QWs suffers from optical loss by absorption, the transition from the 260 nm-wide Ge/SiGe waveguide to the 1 μm-wide active region was then performed using a 1 μm-long transition (second section of the taper). The optical loss was calculated to be only 0.08 dB. In this paper, both section losses are combined in the "taper loss" term.

These results have been used to estimate the modulator performances which are presented in Table II, III and IV for 10, 15, and 20 QWs, respectively. The comparison of modulator performances was done at a given optical loss including taper and active region losses. Then, each table column corresponds to different active region lengths to achieve a total loss (active region + 2 tapers) of 3, 4, and 5 dB. The ERs reported in the tables take into account the overlap factor between the optical mode and the QW region, and the experimental values of absorption coefficients at 1.31 μm for electric field of 0 and 83 kV/cm reported in Table I. The bias voltage required to achieve an electric field of 83 kV/cm varies from 2.9 to 5 V as a function of the number of QWs, due to the increase in the intrinsic region thickness with the increased number of QWs. It can be noticed

TABLE II
MODULATOR PERFORMANCES: 10 QW

Total device loss	3 dB	4 dB	5 dB
Taper loss	0.31 dB	0.31 dB	0.31 dB
Active region loss	2.4 dB	3.4 dB	4.4 dB
Active region length	49 µm	69 µm	89 µm
Bias voltage	2.9V	2.9V	2.9V
Extinction ratio	5.4 dB	7.7 dB	9.9 dB
Capacitance	88 fF	124 fF	158 fF
Energy consumption	42 fJ/bit	59 fJ/bit	75 fJ/bit

TABLE III
MODULATOR PERFORMANCES: 15 QW

Total device loss	3 dB	4 dB	5 dB
Taper loss	0.44 dB	0.44 dB	0.44 dB
Active region loss	2.12 dB	3.12 dB	4.12 dB
Active region length	31 µm	45 µm	60 µm
Bias voltage	3.9V	3.9V	3.9V
Extinction ratio	4.9 dB	7.2 dB	9.5 dB
Capacitance	65 fF	95 fF	126 fF
Energy consumption	36 fJ/bit	51 fJ/bit	68 fJ/bit

TABLE IV
MODULATOR PERFORMANCES: 20 QW

Total device loss	3 dB	4 dB	5 dB
Taper loss	0.85 dB	0.85 dB	0.85 dB
Active region loss	1.3 dB	2.3 dB	3.3 dB
Active region length	15.3 µm	27 µm	38.8 µm
Bias voltage	5V	5V	5V
Extinction ratio	3 dB	5.3 dB	7.7 dB
Capacitance	32 fF	57 fF	82 fF
Energy consumption	22 fJ/bit	40 fJ/bit	57 fJ/bit

that larger ERs were obtained for 10 QWs, thanks to the longer active region, despite the lower overlap factor with the optical mode in comparison to 15 and 20 QW structures. For example, for a modulator with a total loss lower than 4 dB, the maximum active region length was only 27 μm for 20 periods, while for 10 QWs the length can reach 69 μm. The ER was then increased from 5.3 to 7.7 dB for 20 and 10 QWs, respectively.

The energy consumption per bit was calculated using E/bit = 1/4CV^2, where V is the bias voltage and C the capacitance of the diode calculated from its geometry by a simple parallel plate model and taking into account only the active part of the modulator. Despite a smaller bias voltage required by a thinner intrinsic region of the modulator, a larger energy per bit was obtained for 10 periods due the increased length of the device. However energy consumption was always lower than 100 fJ/bit. As a conclusion, high ER (7.7 dB) and low optical loss (4 dB) can be simultaneously obtained with 10 QWs.

IV. Conclusion

In summary, Ge/SiGe QW waveguide modulators working at 1.3 μm have been studied considering two approaches. 1) A stand-alone modulator based on 20 QW periods was fabricated and characterized for light propagating along the QW planes, i.e., in a waveguide configuration, on top of a thick graded SiGe buffer. An ER of 4 dB with insertion loss of 3 dB was experimentally demonstrated using 4 V swing. 2) Development of the modulator integrated with SOI waveguides was also investigated. After the promising experimental demonstration of QCSE using a thin homogenous buffer, performances of a Ge/SiGe waveguide modulator integrated on an SOI waveguide were theoretically studied. High ER, low loss and energy consumption lower than 100 fJ/bit were theoretically estimated for 10 and 20 GeQW structures.

References

[1] B. Jalali and S. Fathpour, "Silicon photonics," *J. Lightw. Technol.*, vol. 24, no. 12, pp. 4600–4615, 2006.

[2] M. Salib, L. Liao, R. Jones, M. Morse, A. Liu, D. Samara-Rubio, D. Alduino, and M. Paniccia, "Silicon photonics," *Intel Technol. J.*, vol. 8, no. 2, pp. 143–160, 2004.

[3] D. Marris-Morini, C. Baudot, J.-M. Fédéli, G. Rasigade, N. Vulliet, A. Souhaité, M. Ziebell, P. Rivallin, S. Olivier, P. Crozat, X. Le Roux, D. Bouville, S. Menezo, F. Boeuf, and L. Vivien, "Low loss 40 Gbit/s silicon modulator based on interleaved junctions and fabricated on 300 mm SOI wafers," *Opt. Exp.*, vol. 21, no. 19, pp. 22471–22475, 2013.

[4] D. A. B. Miller, "Device requirements for optical interconnects to silicon chips," *Proc. IEEE*, vol. 97, no. 7, pp. 1166–1185, Jul. 2009.

[5] Y. H Kuo, Y. K Lee, Y. Ge, S. Ren, J. E. Roth, T. I. Kamins, D. A. B. Miller, and J. S. Harris, "Strong quantum-confined stark effect in germanium quantum-well structures on silicon," *Nature*, vol. 437, no. 27, pp. 1334–1336, 2005.

[6] P. Chaisakul, D. Marris-Morini, M.-S. Rouifed, G. Isella, D. Chrastina, J. Frigerio, X. Le Roux, S. Edmond, J.-R. Coudevylle, and L. Vivien, "23 GHz Ge/SiGe multiple quantum well electroabsorption modulator," *Opt. Exp.*, vol. 20, no. 3, pp. 3219–3224, 2012.

[7] L. Lever, Z. Ikonic, A. Valavanis, J. Cooper, and R. Kelsall, "Design of Ge-SiGe quantum-confined stark effect electroabsorption heterostructures for CMOS compatible photonics," *J. Lightw. Technol.*, vol. 28, no. 22, pp. 3273–3281, 2010.

[8] R. Schaevitz, E. Edwards, J. Roth, E. Fei, Y. Rong, P. Wahl, T. Kamins, J. Harris, and D. Miller, "Simple electroabsorption calculator for designing 1310 and 1550 nm modulators using germanium quantum wells," *IEEE J. Quantum Electron.*, vol. 48, no. 2, pp. 187–197, Feb. 2012.

[9] M.-S. Rouifed, P. Chaisakul, D. Marris-Morini, J. Frigerio, G. Isella, D. Chrastina, S. Edmond, X. Le Roux, J.-R. Coudevylle, and L. Vivien, "Quantum-confined stark effect at 1.3 μm in Ge/Si0.35Ge0.65 quantum-well structure," *Opt. Lett.*, vol. 37, pp. 3960–3962, 2012.

[10] L. Lever, Y. Hu, M. Myronov, X. Liu, N. Owens, F. Y. Gardes, I. P. Marko, S. J. Sweeney, Z. Ikonić, D. R. Leadley, G. T. Reed, and R. W. Kelsall, "Modulation of the absorption coefficient at 1.3 um in Ge/SiGe multiple quantum well heterostructures on silicon," *Opt. Lett.*, vol. 36, pp. 4158–4160, 2011.

[11] E. Onaran, M. C. Onbasli, A. Yesilyurt, H.-Y. Yu, A. M. Nayfeh, and A. K. Okyay, "Silicon-germanium multi-quantum well photodetectors in the near infrared," *Opt. Exp.*, vol. 20, no. 7, pp. 7608–7615, Mar. 2012.

[12] J. E. Roth, O. Fidaner, E. H. Edwards, R. K. Schaevitz, Y.-H. Kuo, N. C. Helman, T. I. Kamins, J. S. Harris, and D. A. B. Miller, "C-band side-entry Ge quantum-well electroabsorption modulator on SOI operating at 1 V swing," *Electron. Lett.*, vol. 44, no. 1, pp. 49–50, 2008.

[13] R. Schaevitz, D. Ly-Gagnon, J. Roth, E. Edwards, and D. Miller, "Indirect absorption in germanium quantum wells," *AIP Advances*, vol. 1, pp. 032164-1–032164-12, 2011.

[14] G. Isella, D. Chrastina, B. Rössner, T. Hackbarth, H.-J. Herzog, U. König, and H. von Känel, "Low-energy plasma-enhanced chemical vapor deposition for strained Si and Ge heterostructures and devices," *Solid State Electron.*, vol. 48, pp. 1317–1323, 2004.

[15] P. Chaisakul, D. Marris-Morini, G. Isella, D. Chrastina, X. Le Roux, S. Edmond, J.-R. Coudevylle, E. Cassan, and L. Vivien, "Polarization dependence of quantum-confined stark effect in Ge/SiGe quantum well planar waveguides," *Opt. Lett.*, vol. 36, no. 10, pp. 1794–1796, 2011.

[16] H.-H. Chang, A. Fang, M. Sysak, H. Park, R. Jones, O. Cohen, O. Raday, M. Paniccia, and J. Bowers, "1310 nm silicon evanescent laser," *Opt. Exp.*, vol. 15, no. 18, pp. 11466–11471, 2007.

[17] S. Ren, Y. Rong, S. Claussen, R. Schaevitz, T. Kamins, J. Harris, and D. Miller, "Ge/SiGe quantum well waveguide modulator monolithically integrated with SOI waveguides," *IEEE Photon. Technol. Lett.*, vol. 24, no. 6, pp. 461–463, Mar. 2012.

[18] L. Lever, Z. Ikonic, and R. Kelsall, "Adiabatic mode coupling between SiGe photonic devices and SOI waveguides," *Opt. Exp.*, vol. 20, no. 28, pp. 29500–29506, 2012.

[19] E. Hedwards, L. Lever, E. Fei, T. Kamins, Z. Ikonic, J. Harris, R. Kelsall, and D. Miller, "Low-voltage broad-band electroabsoption from thin Ge/SiGe quantum wells epitaxially grown on silicon," *Opt. Exp.*, vol. 21, no. 1, pp. 867–876, 2013.

[20] P. Chaisakul, D. Marris-Morini, G. Isella, D. Chrastina, X. Le Roux, E. Gatti, S. Edmond, J. Osmond, E. Cassan, and L. Vivien, "Quantum-confined Stark effect measurements in Ge/SiGe quantum-well structures," *Opt. Lett.*, vol. 35, no. 17, pp. 2913–2915, 2010.

[21] Photon Design software. (2013). [Online]. Available: www.photond.com.